Journal of Soft Computing in Civil Engineering 7-4 (2023) 72-92

Contents lists available at SCCE

Journal of Soft Computing in Civil Engineering

Journal homepage: www.jsoftcivil.com

Finding Optimum Parameters of Passive Tuned Mass Damper by PSO, WOA, and Hybrid PSO-WOA (HPW) Algorithms

Mohammadreza Mashayekhi[1*], Alireza Shirpour[2], Reza Sadeghi[3]

1. Assistant Professor, Department of Civil Engineering, K.N. Toosi University of Technology, Tehran, Iran
2. Ph.D. Candidate, Department of Civil Engineering, K.N. Toosi University of Technology, Tehran, Iran
3. Ph.D. Student, Department of Civil Engineering, K.N. Toosi University of Technology, Tehran, Iran

Corresponding author: *m.mashayekhi@kntu.ac.ir*

https://doi.org/10.22115/SCCE.2023.352340.1489

ARTICLE INFO

Article history:
Received: 18 July 2022
Revised: 03 April 2023
Accepted: 04 April 2023

Keywords:
Tuned mass damper;
Optimal parameters;
Particle swarm optimization (PSO) algorithm;
Whale optimization algorithm (WOA);
Hybrid PSO-WOA (HPW);
State space equations.

ABSTRACT

Using a tuned mass damper (TMD) is one of the passive methods of controlling structural vibrations. This energy absorption system has a mass, a spring, and a damper attaching to the main structure and vibrating with it, reducing the dynamic response of the structure by preventing the intensification. Therefore, finding optimal parameters is one of the main essential issues in the study and design of tuned mass dampers. This study investigates the optimization of parameters of an adjusted mass damper to reduce the displacement and relative response of a multi-story structural system equipped with this damper. For this purpose, a 10-story frame with similar properties on each floor and a 10-story frame with different properties on each floor were modeled under seismic loading in OpenSees software. The optimum parameters were extracted by Matlab software, using the particle swarm optimization (PSO) algorithm, whale optimization algorithm (WOA), and the combination of these two algorithms (Hybrid PSO-WOA) and state space equations controlled the results. Comparing the results with the methods presented by other researchers showed that the proposed methods have good performance and are recommended as approximate and rapid methods for the optimal design of these dampers.

How to cite this article: Mashayekhi M, Shirpour A, Sadeghi R. Finding optimum parameters of passive tuned mass damper by PSO, WOA, and hybrid PSO-WOA (HPW) algorithms. J Soft Comput Civ Eng 2023;7(4):72–92. https://doi.org/10.22115/scce.2023.352340.1489

1. Introduction

In recent years, there has been a tendency to control the seismic behavior of structures with vibrational absorption tools such as seismic base isolators, viscose dampers, friction dampers, and pendulum dampers. A Tuned Mass Damper (TMD) has a mass, a spring, and a damper that is added to the main structure and vibrates with the structure. The TMD's frequency is tuned in resonance with the frequency of the main structure, so a large amount of the structural vibrating energy is transferred to the TMD. Frahm [1] reported the first study on the TMD to control the vibrations of the ship's lounge, which invented a device for damping resonant vibrations in 1911. This device was effective only when the frequency of the TMD was close to the excitation frequency. The main weakness in this device's use is that the TMD's inherent damping is ignored. Ormondroyd [2] updated this old type by adding a viscose damper to the regulated TMD and acquired good results. Den Hartog [3] developed several techniques that could be only used for single-degree-of-freedom systems to optimize damper parameters, including frequency and damping ratios of TMD. In a different method presented by Warburton and Ayorinde [4], if a system's natural frequencies are separated, an SDOF can be used to design the parameters of TMD. Warburton [5] presented a newly regulated damper that estimated the effects of harmonic loading and random white noise in an SDOF. Villaverde et al. [6] found that the optimal performance of TMDs is achieved when the damping ratio of the two primary modes is equal. Other methods have been suggested to improve the TMD performance [7–9].

In recent decades, metaheuristic algorithms have been used to solve and optimize engineering problems. These algorithms are particularly effective for problems in which the definitive solution is complex or unavailable. An example of these algorithms is the genetic algorithm [10,11], the particle swarm algorithm [12], the harmony search algorithm [13], and the charged system search algorithm [14]. Recently, these developed metaheuristic algorithms are used to solve many engineering problems. For example, Babaei et al. [15] employed NSGA-II algorithm to optimize MR semi-active control systems. Ghiasi et al. [16] utilized the invasive weed algorithm to optimize the dimensions of the Koyna weight concrete dam in India, intending to achieve optimal concrete consumption.

The use of metaheuristic algorithms to optimize the parameters of TMD was initially expressed by Hadi and Arfiadi [17]. Lee et al. [18] presented a numerical method that ultimately minimized system responses in the frequency domain. In another study, harmony search algorithm was used as an optimization method by Bekdas et al. [19]. Their study estimated the optimal parameters of TMD by assuming the structure under harmonic loading. Araz et al. [20] proposed a methodology for the optimization of double TMDs of installed on the top floor of a building under seismic loads. Chowdhury et al. [21] used H_2 and H_∞ optimization techniques for optimized system parameters of the negative stiffness inertial amplifier tuned mass dampers (NSIA-TMD). Khatibinia et al. [22] found the optimum design of a TMD for a 10-story inelastic steel moment-resisting frame (SMRF) using the passive congregation particle swarm and grey wolf optimization techniques. Domizio et al. [23] evaluated the performance of the three optimal

TMD configurations on three SDOF structures with different fundamental periods subjected to a set of far-field records and a set of near-fault ground motions with strong velocity pulses.

This research investigates the optimization of passive mass damper parameters (TMD) to reduce dynamic responses of a multi-degree-of-freedom structure with this type of damper under seismic loading. The particle swarm optimization (PSO) algorithm, whale optimization algorithm (WOA), and the combination of these two algorithms (Hybrid PSO-WOA or HPW) have been selected as efficient and effective optimization algorithms for this purpose.

2. Equation of motion

Consider an n-floor shear frame with a mass damper mounted on its roof. The equations of motion of the structural system can be written as Eq. (1).

$$[M]\{\ddot{x}\} + [C]\{\dot{x}\} + [K]\{x\} = -[M]\Gamma\ddot{x}_g \tag{1}$$

That is, $\ddot{x}$, $\dot{x}$, and x, respectively, the vectors of acceleration, velocity, and displacement of the system are multi-degree-of-freedom. Γ is also the impact vector of earth acceleration, a column vector, unit, and co-order with the number of degrees of system freedom. The structures' mass, stiffness, and damping matrices are defined according to Eqs. (2), (3), and (4) [24].

$$[M] = diag\,[m_1, m_2 \ \ldots \ m_N, m_d] \tag{2}$$

$$[C] = \begin{bmatrix} (c_1+c_2) & -c_2 & & & & & \\ -c_2 & (c_1+c_2) & -c_3 & & & & \\ & -c_3 & . & . & & & \\ & & . & . & . & & \\ & & & . & . & -c_n & \\ & & & & -c_n & (c_n+c_d) & -c_d \\ & & & & & -c_d & c_d \end{bmatrix} \tag{3}$$

$$[K] = \begin{bmatrix} (k_1+k_2) & -k_2 & & & & & \\ -k_2 & (k_1+k_2) & -k_3 & & & & \\ & -k_3 & . & . & & & \\ & & . & . & . & & \\ & & & . & . & -k_n & \\ & & & & -k_n & (k_n+k_d) & -k_d \\ & & & & & -k_d & k_d \end{bmatrix} \tag{4}$$

m_i, k_i and c_i are the mass, stiffness, and damping coefficients of floor i ($i = 1,2,\ldots,n$), m_d, k_d, and c_d, respectively, TMD's mass, damping, and stiffness. There are two methods for determining the system response: the time integration method and using state-space equations. Equations of motion can be converted into a set of state-space equations according to Eqs. (5) and (6):

$$\{\dot{Z}\} = [A]\{Z\} + [B]\{F\} \tag{5}$$

$$\{Y\} = [C]\{Z\} + [D]\{F\} \tag{6}$$

The parameters are determined as equations Eqs. (7) to (12):

$$\{Z\} = \begin{Bmatrix} \{x\}_{(n+1)(1)} \\ \{\ddot{x}\}_{(n+1)(1)} \end{Bmatrix}_{(2n+2)(1)} \tag{7}$$

$$[A] = \begin{bmatrix} [0]_{(n+1)(n+1)} & I_{(n+1)(n+1)} \\ -M^{-1}K & -M^{-1}C \end{bmatrix}_{(2n+2)(2n+2)} \tag{8}$$

$$[B] = \begin{bmatrix} [0]_{(n+1)(n+1)} \\ [M]_{(n+1)(n+1)} \end{bmatrix}_{(2n+2)(n+1)} \tag{9}$$

$$\{F\} = -[M]\Gamma\ddot{x}_g \tag{10}$$

$$[C] = [I_{(n+1)(n+1)} \quad [0]_{(n+1)(n+1)}]_{(n+1)(2n+2)} \tag{11}$$

$$[D] = \left[[0]_{(n+1)(n+1)}\right]_{(n+1)(n+1)} \tag{12}$$

$[0]$ and $[I]$ are zero and identity matrices, respectively. When values shown in the above equations are defined, iterative solutions can be used to determine the system response with different loading types, such as seismic excitation.

3. Particle swarm optimization (PSO) algorithm

The particle swarm optimization (PSO) algorithm is a metaheuristic algorithm proposed by Russell Ebrahatt and James Kennedy in 1995. This algorithm works so that a group of particles is randomly distributed in the search space, and their responses are determined. Then, the current position information, the best position in which the particle is located (Pbest), and the best position discovered in the whole particle (Gbest) are recorded. This data is used to determine and modify the new position and velocity of particles (Fig. 1). This step is repeated several times to get the best answer. In each step, the algorithm updates each particle's new velocity and position according to Eqs. (13) and (14) after finding the two Pbest and Gbest values from the previous step. This procedure will continue until the termination conditions (time limit, maximum number of repetitions, and error limits) [12].

$$v_i(t+1) = \omega v_i(t) + c_1 r_1(Pbest_i(t) - x_i(t)) + c_2 r_2(Gbest_i(t) - x_i(t)) \tag{13}$$

$$x_i(t+1) = x_i(t) + v_i(t+1) \tag{14}$$

That $v_i(t)$ and $x_i(t)$ respectively is the velocity and position of the *i*-particles in the *t* repetition. r_1 and r_2 random numbers are between zero and one. c_1 and c_2 constants are called PSO algorithm acceleration coefficients, and ω is the weighted coefficient of inertia, which increasing iterations reduces its value from one to zero. The particle optimization algorithm flowchart is presented in Fig. 2.

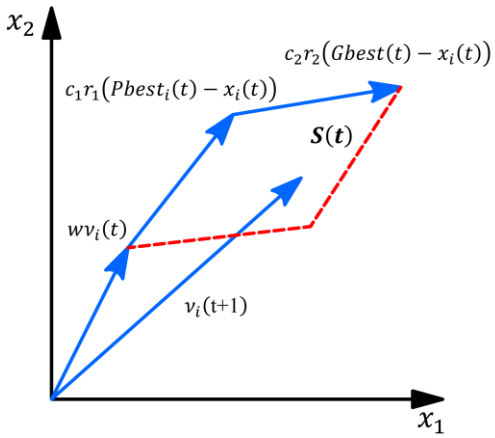

Fig. 1. Particle swarm optimization (PSO) algorithm.

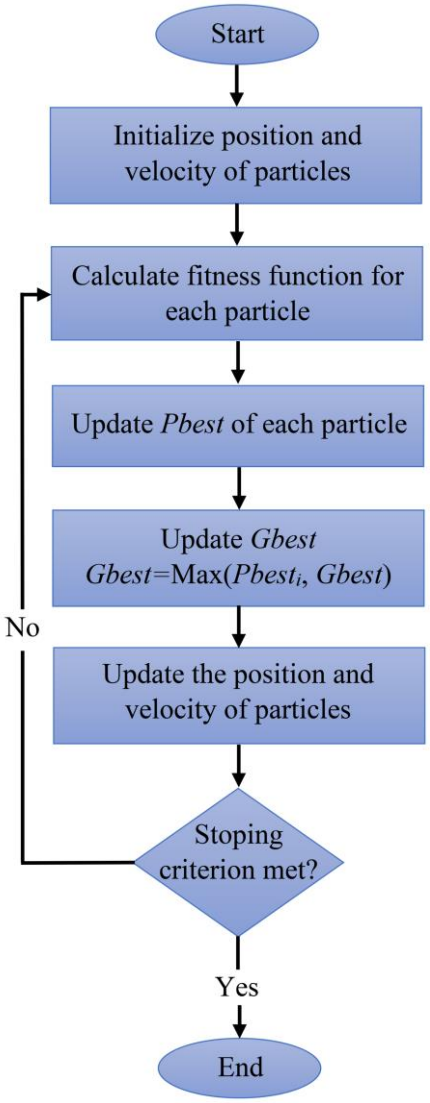

Fig. 2. Particle optimization algorithm flowchart.

4. Whale optimization algorithm (WOA)

This algorithm was proposed by Mirjalili and Lewis [25]. The most exciting thing about whales is their specific hunting method. This exploratory behavior is known as the bubble-net feeding method. Exploration and hunting are accomplished by creating index bubbles along a circle or paths. This feeding behavior is performed by placing specific bubbles in spiral shapes, according to Fig. 3.

Whales can identify and surround the hunting site. The WOA algorithm assumes that the best candidate solution at the moment is to hunt the target or be close to the desired state. After the best search agent is identified, other search agents try to update their location relative to the best search agent. The whale swims around the prey along a contractile circle and simultaneously in a spiral-shaped path. To model this behavior, at the same time, it is assumed that the whale with a 50 percent probability chooses between the mechanism of shrinking the siege or the spiral model to update the position of the whales during optimization (where the random numerical p is between 0 and 1) if $p < 0.5$, the mechanism for shrinking the siege is used according to the following equations.

$$\vec{D} = \left|\vec{C}.\vec{X}^*(t) - \vec{X}(t)\right| \tag{15}$$

$$\vec{X}(t+1) = \vec{X}^*(t) - \vec{A}\vec{D} \tag{16}$$

Where $\vec{A}$ and $\vec{C}$ are determined based on the following equations:

$$\vec{A} = 2\vec{a}.\vec{r} - \vec{a} \tag{17}$$

$$\vec{\mathrm{C}} = 2.\vec{\mathrm{r}} \tag{18}$$

a decrease linearly from 2 to 0 during repetitions, and r is a random vector at a distance of 0 to 1 (Fig. 4). If the value $\left|\vec{A}\right|$ is larger than one, the Eqs. (19) and (20) will replace with Eqs. (15) and (16):

$$\vec{D} = \left|\vec{C}.\vec{X}_{rand}(t) - \vec{X}(t)\right| \tag{19}$$

$$\vec{X}(t+1) = \vec{X}_{rand}(t) - \vec{A}.\vec{D} \tag{20}$$

If $p \geq 0.5$, the spiral position update method (Fig. 5) is used according to the following equations:

$$\vec{D}' = \left|\vec{X}^*(t) - \vec{X}(t)\right| \tag{21}$$

$$\vec{X}(t+1) = \vec{D}'.e^{bl}.cos(2\pi l) + \vec{X}^*(t) \tag{22}$$

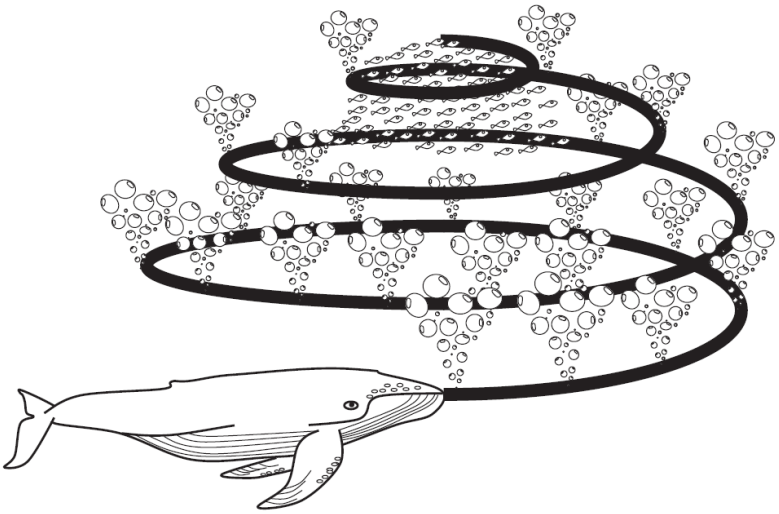

Fig. 3. Bubble-net feeding behavior of humpback whales [25].

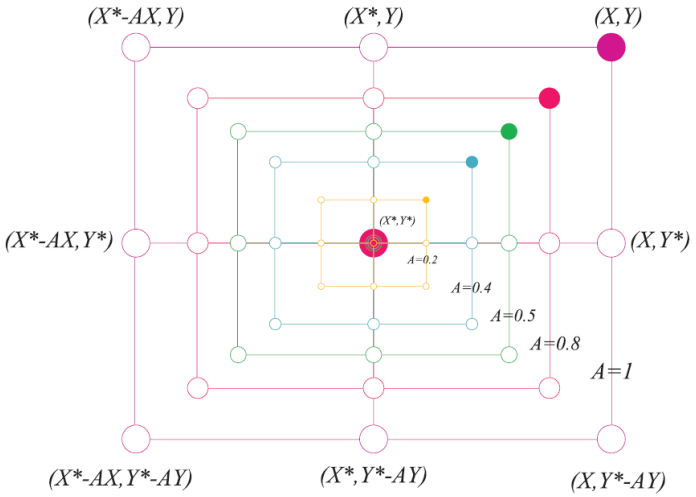

Fig. 4. Shrinking encircling mechanism [25].

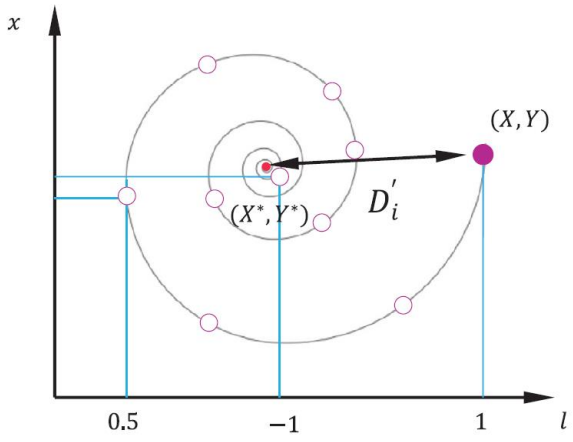

Fig. 5. Spiral updating position [25].

5. Proposed the Hybrid PSO-WOA (HPW) algorithm

In this section, a hybrid algorithm based on the combination of the PSO algorithm and the WOA algorithm is presented. In the PSO algorithm, the position of particles is updated based on either the best solution found for the particle and the best solution found for all particles. On the other hand, in the WOA algorithm, only the best solution found for all whales is used to update whales' positions. These two different features together may result in a more accurate method that is more efficient than either of the two methods alone. The basis of the proposed method is that after performing PSO operators on the particles and updating the best solution of all particles, all particles are considered as whales for applying the WOA method. Then, all the solutions should be updated according to the WOA algorithm. The best solution for each particle and the best solution between all particles are updated again. At the current stage, it is checked that whether the convergence conditions are satisfied or not. In the case that convergence is not occurred, the current solutions are given as particles to the PSO algorithm, and the mentioned process is repeated again. This process is continued until the converge condition is satisfied. The schematic flowchart for the proposed method is shown in Fig. 6.

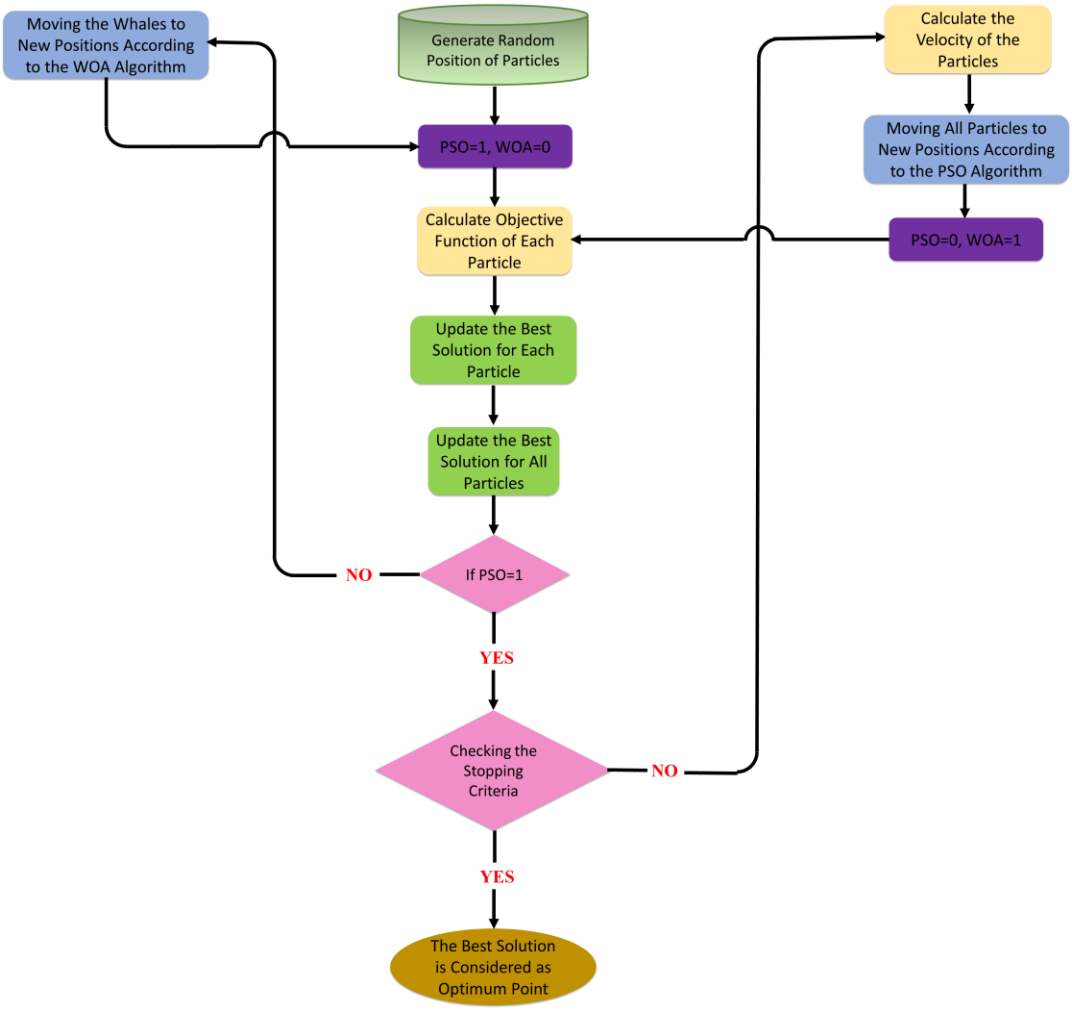

Fig. 6. The flowchart of the proposed hybrid PSO-WOA (HPW) algorithm.

6. The optimum parameters of passive tuned mass damper

In this research, the system's response is obtained using the transient integration methods in OpenSees and controlled by the state-space equation. In this section, both methods are first explained, and then the responses of two numerical examples are extracted using them and compared with the results of previous studies.

6.1. The state-space equations

In this study, TMD's optimal stiffness and damping parameters are calculated by considering a constant mass for TMD. Then, the TMD's optimal mass is obtained according to the other two parameters. The optimization process minimizes the maximum floor drift relative to the ground when the structure is excited under an earthquake. This procedure can be done by adding a transfer function between changing the upstairs location and the ground acceleration to the objective function. Generally, the transfer function is defined as a criterion for evaluating the number of input components transferred to the system. By taking the Laplace conversion (with zero initial conditions) from the space system, we have the state defined in Eqs.(23) and (24):

$$\dot{Z}(t) = AZ(t) + BF(t) \xrightarrow{L} sZ(s) = AZ(s) + BF(s) \tag{23}$$

$$Y(t) = CZ(t) + DF(t) \xrightarrow{L} Y(s) = CZ(s) + DF(s) \tag{24}$$

By solving these equations:

$$Z(s) = (sI - A)^{-1}BF(s) \tag{25}$$

The transfer function was defined as an output Laplace transformation adjusted to the Laplace transform of the input function (external forces).

$$T.F = \frac{Y(s)}{F(s)} = C(sI - A)^{-1}B + D \tag{26}$$

Where, $T.F$ is the transfer function between the input and output of the system, which can be used for displacement or acceleration, it should be noted that, as can be seen in Eq. (26), the transfer function is independent of the type of output component and is considered to be an inherent feature of the system. Considering the force entered into the first floor as input and displacement of the first floor of the MDOF as an output (in the transmission function in both controlled and uncontrolled) and displacement ratio (in both controlled and uncontrolled) as a factor for controlling the behavior of the structure, the objective function can be defined as follows:

$$Objective\ function = \frac{max(TF_1\ with\ TMD)}{max(TF_1\ without\ TMD)} + \frac{max|x_1\ with\ TMD|}{max|x_1\ without\ TMD|} \tag{27}$$

6.2. The transient integration method in OpenSees

The structures are initially modeled in the OpenSees software to extract the systems' responses using the transient integration method. For this purpose, a ten-story shear building with one span

is considered. In this building, the height of columns and span width were assumed to be 3 meters. In the first example, a 10-story frame with similar properties on each floor, and in the second example, a 10-story shear frame with different properties on each floor are investigated. Elastic beam-column element is also used to model the samples. The beam of the floors is assumed to be rigid, and using the stiffness presented in previous studies and the relation $K = 24EIc/Lc^3$, the columns' characteristics are entered into the software [26]. Uniaxial materials viscous and element two node link are used to consider damping in floors. The schematic of the structure used is depicted in Fig. 7. In the transient integration method, the ratio of maximum displacements of the top floor of the frame with and without TMD is minimized for the optimization objective.

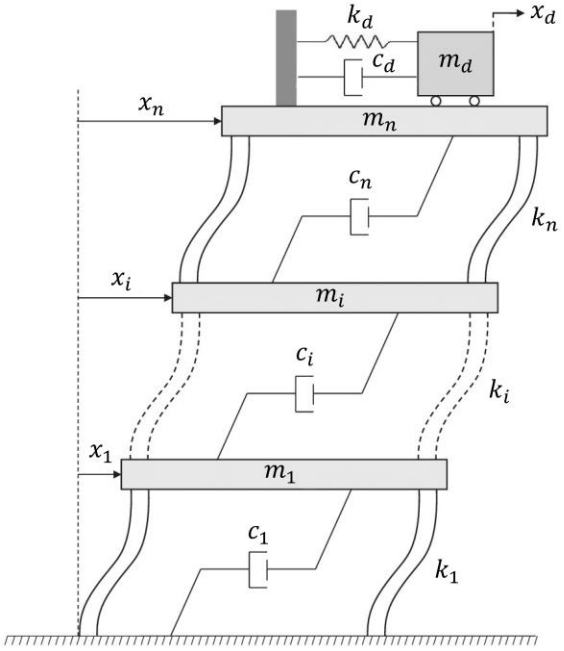

Fig. 7. The n-story shear building with the TMD.

6.3. Numerical examples

6.3.1. Example 1

This example investigates a ten-story frame with a TMD attached to the top floor and under seismic loading (El Centro earthquake). The characteristics of this building are shown in Table 1. TMD mass is taken at 108 tons. TMD stiffness and damping values are defined as optimization algorithm variables. The lower and upper bounds of stiffness are 0 and 5000 kN/m. Also, the lower and upper bounds of the damping coefficients are 0 and 1000 kN.s/m.

The results of the genetic algorithm (GA) [17], the method presented by Lee et al. [18], the search of the charged system (CSS) [26], and the three methods presented in this study are demonstrated in Table 2. According to this table, the WOA and HPW algorithms have predicted the lowest value among the optimal values for c_d and k_d. The optimal value for c_d and k_d in the PSO algorithm is 173.86 and 122.91% higher than the values obtained from the WOA algorithm, respectively. The optimal values of WOA and HPW algorithms are also close to each other.

Table 1
Properties of the building for Example 1.

Story	Mass (ton)	Stiffness (kN/m)	Damping (kN.s/m)
1	360	650000	6200
2	360	650000	6200
3	360	650000	6200
4	360	650000	6200
5	360	650000	6200
6	360	650000	6200
7	360	650000	6200
8	360	650000	6200
9	360	650000	6200
10	360	650000	6200

Table 2
Stiffness and damping coefficient of the TMD for Example 1.

TMD parameters	Optimum values					
	Ref. [17]	Ref. [18]	Ref. [26]	PSO	WOA	HPW
c_d (kN.s/m)	151.50	271.79	88.70	117.50	67.58	70.08
k_d (kN/m)	3750	4127	4208	4136	3365	3336

The maximum absolute displacement of each floor relative to the ground (in both controlled and uncontrolled) is summarized in Table 3. The percentage of displacement reduction is shown in Table 4. To better understand the results of Table 4, these results are presented again in Fig. 8. The results show that by using a TMD attached to the top floor in a ten-story shear frame, the maximum absolute displacement is reduced. The amount of reduction predicted for absolute displacement by PSO, WOA, and HPW algorithms are equal to 37.21, 38.54%, and 38.85, respectively. The changes in the objective function versus the number of iterations for the first example come in three optimization algorithms in Fig. 9(a) to 9(c). As can be observed, the PSO, WOA, and HPW algorithms have converged to the optimum solution before 40, 90, and 70 iterations, respectively.

The time history displacement of the structure from the first to the tenth floor is depicted in Fig. 10(a) to 10(j). When the optimum values of TMD stiffness and damping coefficient are determined, the system performance can now be improved by changing the mass of TMD, which was initially selected at 108 tons. For this purpose, the system response should be investigated by applying changes in the range of 90 to 116 tons (with the same desired stiffness values and damping coefficient as previously determined). The results of these changes for the PSO method are shown in Table 5. According to Table 5, increasing the TMD mass from 90 to 100 will lead to a decrease in the maximum displacement. For example, the PSO algorithm has predicted that the mass increase from 90 to 100 tons and the maximum displacement on the top floor has decreased by 8.8%, but increasing the mass from 100 to 116 tons has led to an increase in the maximum displacement.

Table 3
Maximum absolute displacement of each floor relative to the ground (m).

Story	Without TMD	With TMD					
		Ref. [17]	Ref. [18]	Ref. [26]	PSO	WOA	HPW
1	0.031	0.019	0.020	0.018	0.0191	0.0185	0.0181
2	0.060	0.037	0.039	0.036	0.0375	0.0361	0.0355
3	0.087	0.058	0.057	0.052	0.0547	0.0524	0.0519
4	0.112	0.068	0.073	0.068	0.0682	0.0673	0.0668
5	0.133	0.082	0.087	0.082	0.0826	0.0812	0.0808
6	0.151	0.094	0.099	0.095	0.0946	0.0933	0.0934
7	0.166	0.104	0.108	0.105	0.1044	0.1033	0.1035
8	0.177	0.113	0.117	0.113	0.1139	0.1110	0.1112
9	0.184	0.119	0.123	0.119	0.1191	0.1164	0.1167
10	0.188	0.122	0.126	0.122	0.1222	0.1191	0.1192

Table 4
Percentage of displacement reduction (%).

Story	Ref. [17]	Ref. [18]	Ref. [26]	PSO	WOA	HPW
1	38.71	35.48	40.32	38.70	40.32	41.61
2	38.33	35.00	39.67	38.33	39.83	40.83
3	33.33	34.48	39.65	36.89	39.77	40.34
4	39.29	34.82	39.11	39.28	39.91	40.36
5	38.35	34.59	37.97	37.59	38.95	39.25
6	37.75	34.44	37.09	37.08	38.21	38.15
7	37.35	34.94	36.39	37.34	37.77	37.65
8	36.16	33.90	35.69	35.59	37.29	37.18
9	35.33	33.15	35.00	35.32	36.74	36.58
10	35.11	32.98	34.84	35.10	36.65	36.60
Mean	36.97	34.38	35.57	37.21	38.54	38.85

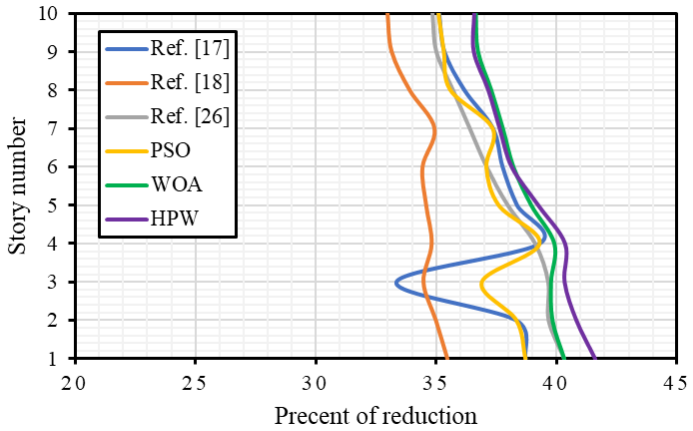

Fig. 8. Percentage of displacement reduction.

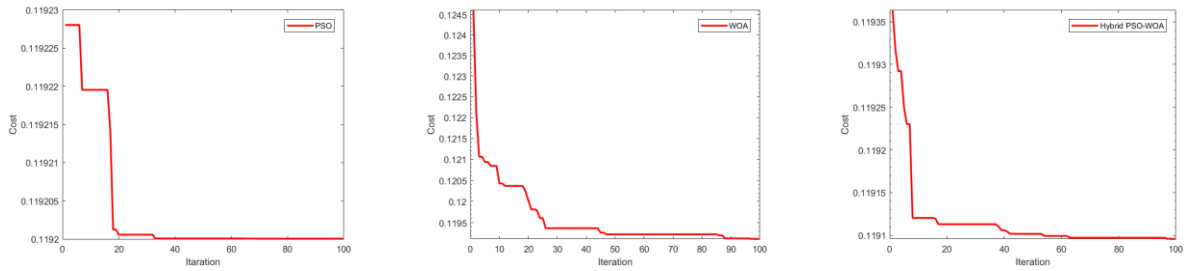

(a) (b) (c)

Fig. 9. Variation of objective function versus the number of iterations. a) PSO, b) WOA, and c) HPW.

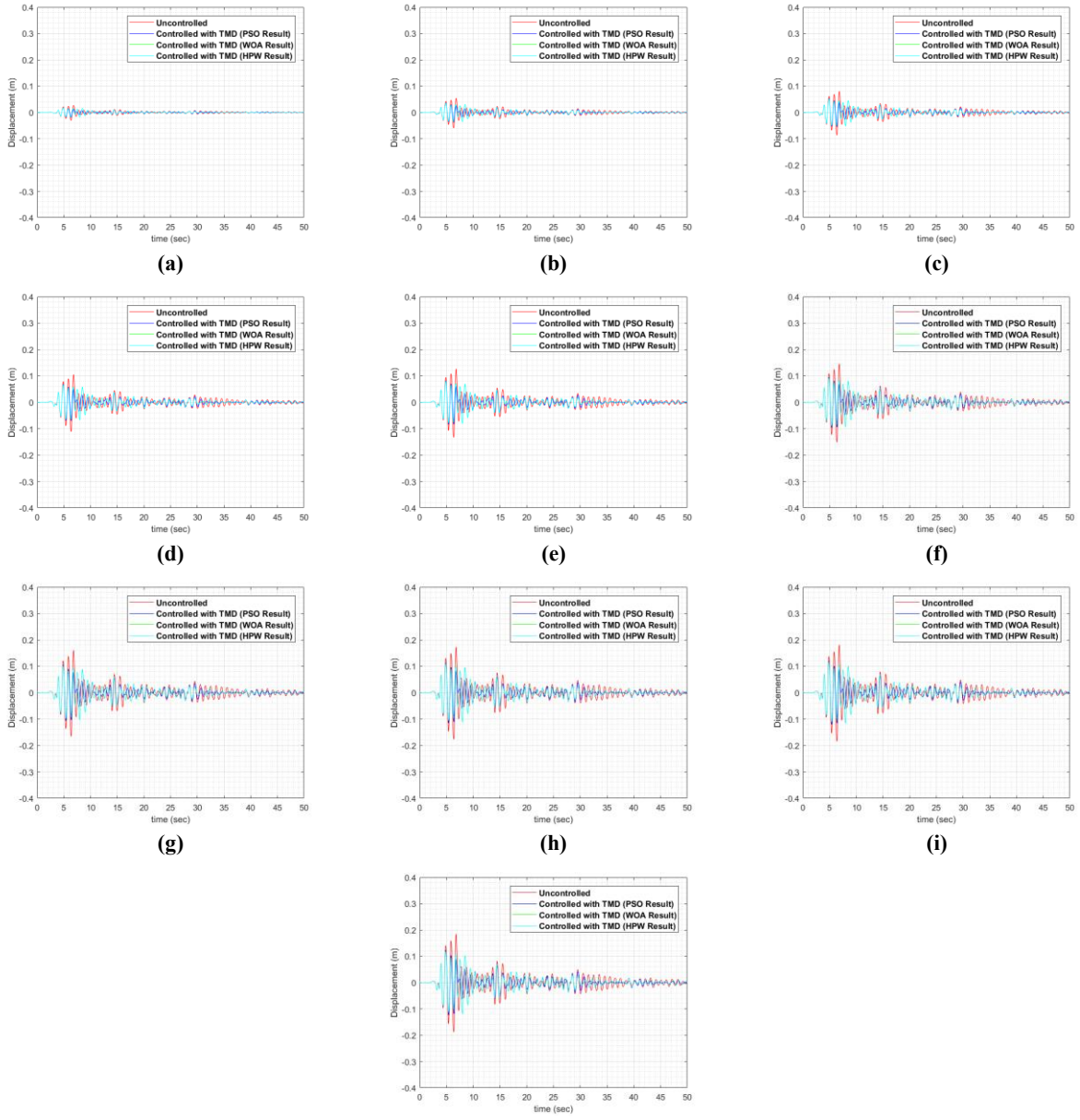

(a) (b) (c)

(d) (e) (f)

(g) (h) (i)

(j)

Fig. 10. Time history displacement during the El Centro excitation. a) first floor, b) second floor, c) third floor, d) 4th floor, e) 5th floor, f) 6th floor, g) 7th floor, h) 8th floor, i) 9th floor, j) top floor.

Table 5
Comparison of maximum displacement (in meters) of each story to the ground under El Centro earthquake with different amounts of TMD mass (PSO algorithm).

Story	TMD mass (ton)						
	90	96	100	104	108	112	116
1	0.018	0.017	0.016	0.017	0.019	0.019	0.020
2	0.036	0.034	0.033	0.035	0.037	0.039	0.041
3	0.051	0.048	0.047	0.050	0.055	0.056	0.058
4	0.066	0.063	0.062	0.065	0.068	0.073	0.076
5	0.076	0.073	0.072	0.075	0.083	0.085	0.089
6	0.089	0.086	0.085	0.088	0.095	0.100	0.104
7	0.100	0.097	0.095	0.099	0.104	0.111	0.116
8	0.110	0.116	0.104	0.117	0.114	0.122	0.125
9	0.114	0.110	0.108	0.11	0.119	0.125	0.130
10	0.125	0.116	0.114	0.115	0.122	0.130	0.135

The effect of ground motion (GM) record change on the three algorithms' performance was also evaluated in this example. For this purpose, six GM records from the far-field records provided in FEMA P695 methodology [27] were selected according to Table 6. These GM records were scaled based on the first-mode period ($Sa(T_1)$ scaling method), considering the El Centro earthquake as the target spectral acceleration.

Table 6
FEMA P695 far-field ground motion record set [27]

ID No.	Event name	Year	Magnitude	Station	Site class (NEHRP)	PGA_{max} (g)	PGV_{max} (cm/s)
1	Northridge	1994	6.7	Beverly hills	D	0.52	63
2	Duzce, Turkey	1999	7.1	Bolu	D	0.82	62
3	Hector Mine	1999	7.1	Hector	C	0.34	42
4	Kobe, Japan	1995	6.9	Nishi-Akashi	C	0.51	37
5	Landers	1992	7.3	Yermo Fire Station	D	0.24	52
6	Manjil, Iran	1990	7.4	Abbar	C	0.51	54

The maximum absolute displacement of each floor relative to the ground (in both controlled and uncontrolled) under these three GM records is summarized in Table 7. Also, the percentage of displacement reduction is shown in Table 8. For clearer comprehension of the results, a bar chart was drawn according to the percentage of displacement reduction provided for each record in Fig.11(a). Additionally, the mean response distribution for the percentage of displacement reduction due to record-to-record (RTR) variability per three algorithms is shown in Fig. 11(b) using lognormal probability distribution functions (PDFs).

Table 7
Maximum absolute displacement of each floor relative to the ground for different far-field GM records (m).

GM records	Case	Story									
		1	2	3	4	5	6	7	8	9	10
Northridge	Without TMD	0.03184	0.06252	0.09150	0.11824	0.14221	0.16294	0.18002	0.19317	0.20212	0.20665
	PSO	0.02101	0.04125	0.06041	0.07817	0.09424	0.10836	0.12027	0.12977	0.13669	0.14090
	WOA	0.01643	0.03223	0.04703	0.06050	0.07236	0.08273	0.09160	0.09856	0.10351	0.10639
	HPW	0.01633	0.03203	0.04675	0.06015	0.07196	0.08197	0.08995	0.09576	0.09951	0.10224
Duzce, Turkey	Without TMD	0.06490	0.12757	0.18661	0.24087	0.28937	0.33128	0.36597	0.39271	0.41089	0.42008
	PSO	0.04952	0.09786	0.14404	0.18728	0.22669	0.26157	0.29132	0.31553	0.33382	0.34581
	WOA	0.04978	0.09860	0.14539	0.18893	0.22840	0.26322	0.29306	0.31555	0.32981	0.33533
	HPW	0.04933	0.09771	0.14411	0.18726	0.22644	0.26079	0.29036	0.31265	0.32679	0.33228
Hector Mine	Without TMD	0.03643	0.07159	0.10486	0.13563	0.16330	0.18740	0.20746	0.22296	0.23351	0.23886
	PSO	0.01484	0.02937	0.04347	0.05669	0.06872	0.07930	0.08823	0.09538	0.10069	0.10404
	WOA	0.01182	0.02309	0.03365	0.04347	0.05261	0.06105	0.06848	0.07448	0.07873	0.08086
	HPW	0.01177	0.02299	0.03350	0.04327	0.05236	0.06075	0.06811	0.07406	0.07826	0.08037
Kobe, Japan	Without TMD	0.19068	0.37658	0.55568	0.72297	0.87439	1.00629	1.11551	1.19956	1.25660	1.28541
	PSO	0.07116	0.13959	0.20381	0.26267	0.31489	0.35923	0.39465	0.42037	0.43618	0.44136
	WOA	0.13021	0.25607	0.37477	0.48373	0.58054	0.66309	0.72939	0.77775	0.80698	0.81635
	HPW	0.13459	0.26469	0.38744	0.50020	0.60062	0.68625	0.75505	0.80536	0.83594	0.84602
Landers	Without TMD	0.02835	0.05581	0.08179	0.10574	0.12720	0.14576	0.16107	0.17284	0.18089	0.18502
	PSO	0.01593	0.03127	0.04578	0.05921	0.07140	0.08212	0.09118	0.09837	0.10349	0.10637
	WOA	0.01592	0.03130	0.04587	0.05940	0.07165	0.08239	0.09141	0.09855	0.10354	0.10624
	HPW	0.01534	0.03015	0.04419	0.05722	0.06902	0.07936	0.08804	0.09487	0.09967	0.10229
Manjil, Iran	Without TMD	0.02973	0.05810	0.08391	0.10647	0.12599	0.14258	0.15598	0.16543	0.17165	0.17492
	PSO	0.01830	0.03581	0.05163	0.06522	0.07650	0.08592	0.09329	0.09863	0.10199	0.10389
	WOA	0.02146	0.04165	0.05947	0.07466	0.08770	0.09876	0.10732	0.11331	0.11820	0.12104
	HPW	0.02158	0.04186	0.05975	0.07506	0.08817	0.09936	0.10804	0.11414	0.11932	0.12218

Table 8
Percentage of displacement reduction for different far-field GM records (%).

GM records	Case	Story										Mean
		1	2	3	4	5	6	7	8	9	10	
Northridge	PSO	34.01	34.02	33.98	33.89	33.73	33.50	33.19	32.82	32.37	31.82	33.33
	WOA	48.40	48.45	48.60	48.83	49.11	49.22	49.11	48.98	48.79	48.52	48.80
	HPW	48.72	48.77	48.91	49.13	49.40	49.69	50.03	50.43	50.77	50.52	49.64
Duzce, Turkey	PSO	23.71	23.29	22.81	22.25	21.66	21.04	20.40	19.65	18.76	17.68	21.13
	WOA	23.30	22.71	22.09	21.56	21.07	20.54	19.92	19.65	19.73	20.18	21.08
	HPW	24.00	23.41	22.78	22.25	21.75	21.28	20.66	20.39	20.47	20.90	21.79
Hector Mine	PSO	59.27	58.97	58.55	58.20	57.92	57.68	57.47	57.22	56.88	56.44	57.86
	WOA	67.54	67.75	67.91	67.95	67.79	67.42	66.99	66.59	66.29	66.15	67.24
	HPW	67.68	67.89	68.05	68.09	67.94	67.58	67.17	66.78	66.48	66.35	67.40
Kobe, Japan	PSO	62.68	62.93	63.32	63.67	63.99	64.30	64.62	64.96	65.29	65.66	64.14
	WOA	31.71	32.00	32.56	33.09	33.61	34.11	34.61	35.16	35.78	36.49	33.91
	HPW	29.42	29.71	30.28	30.81	31.31	31.80	32.31	32.86	33.48	34.18	31.62
Landers	PSO	43.81	43.97	44.03	44.01	43.87	43.66	43.39	43.09	42.79	42.51	43.51
	WOA	43.83	43.92	43.91	43.82	43.67	43.48	43.25	42.98	42.76	42.58	43.42
	HPW	45.89	45.98	45.97	45.88	45.74	45.56	45.34	45.11	44.90	44.71	45.51
Manjil, Iran	PSO	38.45	38.36	38.47	38.74	39.28	39.74	40.19	40.38	40.58	40.61	39.48
	WOA	27.83	28.31	29.13	29.87	30.40	30.73	31.19	31.51	31.14	30.81	30.09
	HPW	27.44	27.94	28.80	29.50	30.02	30.31	30.73	31.01	30.49	30.15	29.64

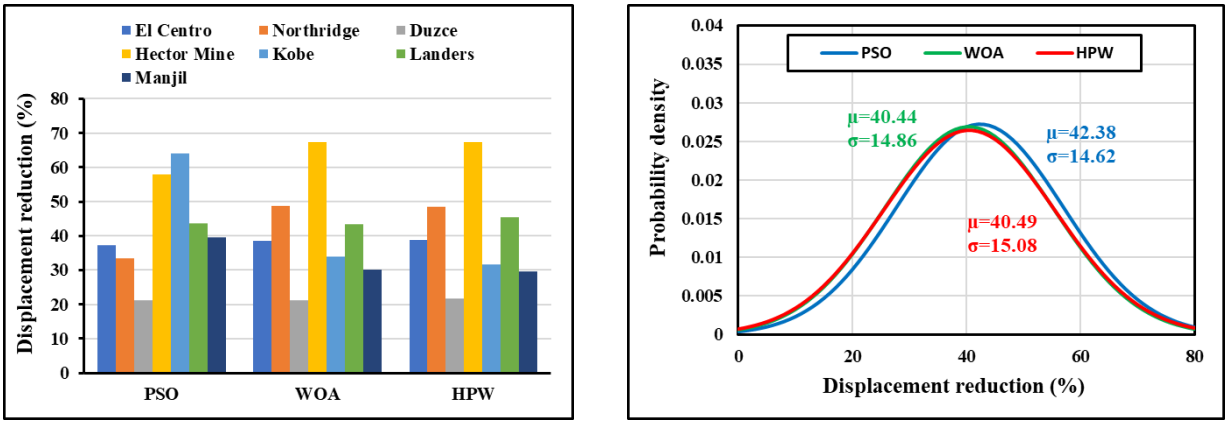

(a) **(b)**

Fig. 11. a) Bar chart of the percentage of displacement reduction, b) Probability distribution functions (PDFs) for the percentage of displacement reduction.

Figure 11(a) shows that using the HPW algorithm in seismic excitation under Northridge, Duzce, Hector Mine, and Landers earthquakes has caused a greater reduction in the displacement of floors than the other two algorithms. As a result, this algorithm has provided more optimum parameters for the passive-tuned mass damper. Figure 11(b) shows that due to the nearly equal extracted responses' standard deviation of all three algorithms, the distribution of the responses is likewise equal, and eventually, RTR variability is nearly the same per three algorithms.

6.3.2. Example 2

This example investigates another 10-story frame with a TMD attached to the top floor and undergoing seismic loading (El Centro earthquake). The properties of this building are shown in Table 9. Like the first example, TMD stiffness and damping values are defined as variables of the optimization algorithm. The lower and upper bounds of stiffness are 0 and 500 kN/m, respectively, and the lower and upper bounds of the damping coefficient are 0 and 150 kN.s/m, respectively. The optimal TMD values estimated in this research and previous research are shown in Table 10. The optimal value of c_d and k_d obtained from the PSO algorithm is 404.76 and 194.78% higher than the optimal value obtained from the WOA algorithm. Like the previous example, the WOA and HPW algorithms have predicted the lowest optimal value of c_d and k_d, and the optimal values of WOA and HPW algorithms are close to each other.

The maximum absolute displacement of each floor relative to the ground (in both controlled and uncontrolled) and the percentage of displacement reduction are shown in Tables 11 and 12, also changes in the objective function versus the number of iterations for the second example in three optimization algorithms are depicted in Fig. 12(a) to 12(c). Also, the time history of floor displacement of the structure from the first floor to the tenth floor is shown in Fig. 13(a) to 13(j). The HPW algorithm has predicted a greater reduction in displacement than the other two algorithms (PSO algorithm, 26.91%, WOA algorithm, 26.88%, and HPW algorithm, 28.09). According to Fig. 12, the PSO, WOA, and HPW algorithms have converged to the optimum solution before 20, 50, and 40 iterations, respectively.

Table 9
Properties of the building for Example 2.

Story	Mass (ton)	Stiffness (kN/m)	Damping (kN.s/m)
1	179	62470	805.863
2	170	52260	674.154
3	161	56140	724.206
4	152	53020	683.958
5	143	49910	643.839
6	134	46790	603.591
7	125	43670	563.095
8	116	40550	523.098
9	107	37430	482.847
10	98	34310	442.592

Table 10
Stiffness and damping coefficient of the TMD for Example 2.

TMD parameters	Optimum values					
	Ref. [28]	Ref. [17]	Ref. [26]	PSO	WOA	HPW
c_d (kN.s/m)	104.4	48.9	30.23	119.85	29.61	25.33
k_d (kN/m)	464.1	437.4	355.76	493.50	253.36	289.87

Table 11
Maximum absolute displacement of each floor relative to the ground (m).

Story	Without TMD	With TMD							
		Ref. [3]	Ref. [6]	Ref. [28]	Ref. [17]	Ref. [26]	PSO	WOA	HPW
1	0.041	0.034	0.036	0.036	0.034	0.030	0.0291	0.0320	0.0303
2	0.088	0.074	0.079	0.077	0.065	0.065	0.0624	0.0687	0.0650
3	0.129	0.106	0.114	0.113	0.094	0.094	0.0923	0.0996	0.0941
4	0.166	0.136	0.147	0.145	0.120	0.120	0.1195	0.1272	0.1206
5	0.197	0.163	0.177	0.172	0.143	0.143	0.1391	0.1497	0.1461
6	0.222	0.187	0.206	0.194	0.163	0.163	0.1552	0.1667	0.1675
7	0.252	0.213	0.236	0.219	0.186	0.186	0.1822	0.1786	0.1849
8	0.286	0.239	0.267	0.245	0.209	0.209	0.2182	0.1928	0.1987
9	0.313	0.261	0.292	0.266	0.229	0.229	0.2441	0.2069	0.2092
10	0.327	0.276	0.310	0.281	0.242	0.242	0.2565	0.2153	0.2171

Table 12
Percentage of displacement reduction (%).

Story	Ref. [3]	Ref. [6]	Ref. [28]	Ref. [17]	Ref. [26]	PSO	WOA	HPW
1	17.07	12.20	12.20	17.07	25.37	29.11	21.95	26.10
2	15.91	10.23	12.50	18.18	25.56	29.10	21.93	26.14
3	17.83	11.63	12.40	18.60	26.67	28.43	22.79	27.05
4	18.07	11.45	12.65	19.28	27.40	28.00	23.37	27.35
5	17.26	10.15	12.69	18.78	27.41	29.41	24.01	25.84
6	15.77	7.21	12.61	17.12	26.35	30.09	25.04	24.55
7	15.48	6.35	13.10	16.67	26.06	27.71	29.12	26.63
8	16.43	6.64	14.34	17.48	26.61	23.70	32.58	30.52
9	16.61	6.71	15.02	17.57	26.54	22.02	33.89	33.16
10	15.60	5.20	14.07	16.82	25.78	21.56	34.15	33.61
Mean	16.60	8.78	13.16	17.76	26.37	26.91	26.88	28.09

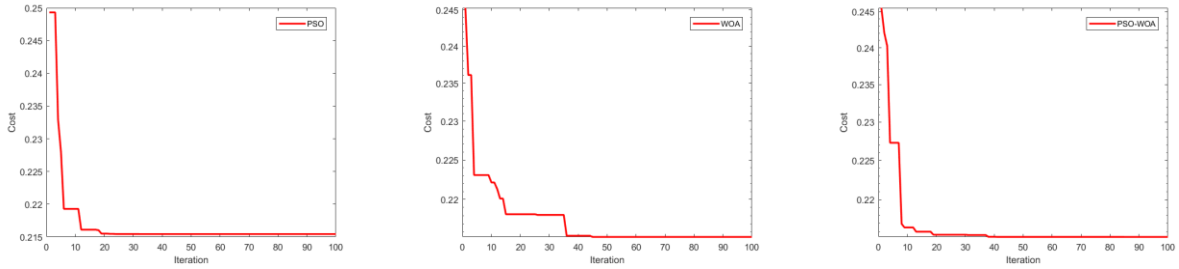

(a) **(b)** **(c)**

Fig. 12. Variation of objective function versus the number of iterations. a) PSO, b) WOA, and c) HPW.

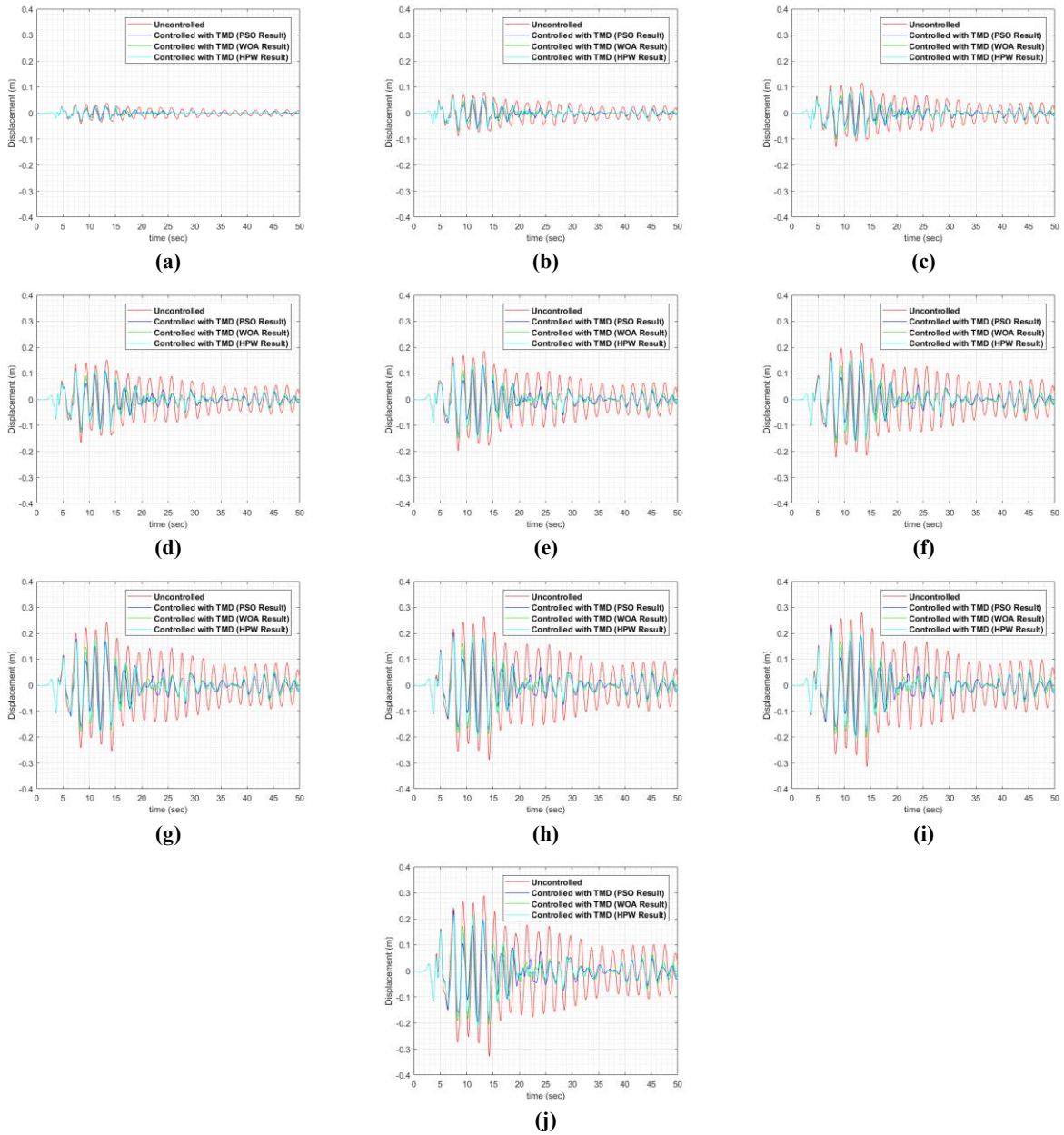

Fig. 13. Time history displacement during the El Centro excitation. a) first floor, b) second floor, c) third floor, d) 4th floor, e) 5th floor, f) 6th floor, g) 7th floor, h) 8th floor, i) 9th floor, j) top floor.

7. Conclusion

The primary purpose of this study was to estimate the optimum parameters of a passive mass damper to reduce the system's response under earthquake loading. The emphasis on the inactive type of TMD damper is because this type of TMD does not delay responding to the system reaction and usually requires lower costs than other types. The particle swarm optimization (PSO) algorithm, whale optimization algorithm (WOA), and the combination of these two algorithms (Hybrid PSO-WOA or HPW) have been used to determine the optimum stiffness and damping of TMD. The system's response was obtained using the transient integration methods in

OpenSees and controlled by the state-space equation. In the first example, a 10-story shear frame with similar properties on each floor, and in the second example, a 10-story shear frame with different properties on each floor under the seismic loading of the El Centro earthquake is presented to demonstrate the effectiveness of the proposed method. The optimal value predicted for c_d and k_d from the PSO algorithm in example 1 is 1.74 and 1.23 times the optimal value predicted by the WOA algorithm, respectively. Also, the optimal value predicted for c_d and k_d from the PSO algorithm in example 2 is 4.05 and 1.98 times the optimal value predicted by the WOA algorithm, respectively. In both examples, the WOA and HPW algorithms have predicted the lowest optimal value of c_d and k_d, and the optimal values of WOA and HPW algorithms are near each other, and the HPW algorithm has predicted a near each other reduction in displacement than the other two algorithms. Moreover, The effect of ground motion (GM) record change on the three algorithms' performance by considering six far-field GM records provided in the FEMA P695 methodology was assessed in the first example. Like the earlier outcomes, the HPW algorithm has provided more optimum parameters for the passive-tuned mass damper, and RTR variability is approximately the same per three algorithms. The practical advantage of using these algorithms, among other metaheuristic optimization algorithms, is that these algorithms have the most uncomplicated relationships and the slightest need for external parameters. The proposed methods have good performance and are recommended as three approximate and rapid methods for the optimal design of these dampers.

Acknowledgments

The authors gratefully acknowledge the useful comments of anonymous reviewers on the draft version of this paper.

Funding

This research received no external funding.

Conflicts of interest

The authors declare no conflict of interest.

References

[1] Frahm H. Device for damping vibrations of bodies. 989,958, 1911.
[2] Ormondroyd J. Theory of the dynamic vibration absorber. Trans ASME 1928;50:9–22.
[3] Hartog DJP. Mechanical vibrations. McGraw-Hill Book Company; 1956.
[4] Warburton GB, Ayorinde EO. Optimum absorber parameters for simple systems. Earthq Eng Struct Dyn 1980;8:197–217.
[5] Warburton GB. Optimum absorber parameters for various combinations of response and excitation parameters. Earthq Eng Struct Dyn 1982;10:381–401.
[6] Villaverde R, Koyama LA. Damped resonant appendages to increase inherent damping in buildings. Earthq Eng Struct Dyn 1993;22:491–507.

[7] Mashayekhi M, Harati M, Estekanchi HE. Development of an alternative PSO-based algorithm for simulation of endurance time excitation functions. Eng Reports 2019:1–15. https://doi.org/10.1002/eng2.12048.

[8] Ghasemof A, Mirtaheri M, Mohammadi RK, Mashayekhi MR. Multi-objective optimal design of steel MRF buildings based on life-cycle cost using a swift algorithm. Structures, vol. 34, Elsevier; 2021, p. 4041–59.

[9] Mashayekhi M, Estekanchi HE, Vafai H. Optimal objective function for simulating endurance time excitations. Sci Iran 2020;27:1728–39. https://doi.org/10.24200/sci.2018.5388.1244.

[10] Holland J. Adaptation in natural and artificial systems 1975.

[11] Golberg DE. Genetic algorithms in search, optimization, and machine learning. Addion Wesley 1989;1989:36.

[12] Kennedy J, Eberhart R. Particle swarm optimization. Proc. IEEE Int. Conf. Neural Netw. IV, 1942–1948., vol. 4, IEEE; 1995, p. 1942–8. https://doi.org/10.1109/ICNN.1995.488968.

[13] Zong Woo Geem, Joong Hoon Kim, Loganathan GV. A New Heuristic Optimization Algorithm: Harmony Search. Simulation 2001;76:60–8. https://doi.org/10.1177/003754970107600201.

[14] Kaveh A, Talatahari S. A novel heuristic optimization method: charged system search. Acta Mech 2010;213:267–89.

[15] Babaei M, Taghaddosi N, Seraji N. Optimal Design of MR Dampers Using NSGA-II Algorithm. J Soft Comput Civ Eng 2023;7:72–92.

[16] Ghiasi V, Alborzi Moghadam M, Koushki M. Optimization of Invasive Weed for Optimal Dimensions of Concrete Gravity Dams. J Soft Comput Civ Eng 2022;6:95–111. https://doi.org/10.22115/scce.2022.340697.1432.

[17] Hadi MNS, Arfiadi Y. Optimum design of absorber for MDOF structures. J Struct Eng 1998;124:1272–80.

[18] Lee C-L, Chen Y-T, Chung L-L, Wang Y-P. Optimal design theories and applications of tuned mass dampers. Eng Struct 2006;28:43–53.

[19] Bekdaş G, Nigdeli SM. Estimating optimum parameters of tuned mass dampers using harmony search. Eng Struct 2011;33:2716–23.

[20] Araz O, Elias S, Kablan F. Seismic-induced vibration control of a multi-story building with double tuned mass dampers considering soil-structure interaction. Soil Dyn Earthq Eng 2023;166:107765.

[21] Chowdhury S, Banerjee A, Adhikari S. The optimal design of dynamic systems with negative stiffness inertial amplifier tuned mass dampers. Appl Math Model 2023;114:694–721.

[22] Khatibinia M, Akbari S, Yazdani H, Gharehbaghi S. Damage-based optimal control of steel moment-resisting frames equipped with tuned mass dampers. J Vib Control 2023:10775463221149462.

[23] Domizio M, Garrido H, Ambrosini D. Single and multiple TMD optimization to control seismic response of nonlinear structures. Eng Struct 2022;252:113667.

[24] Chopra AK. Dynamics of structures: Theory and applications to earthquake engineering. 4 edition. Pearson; 1995.

[25] Mirjalili S, Lewis A. The Whale Optimization Algorithm. Adv Eng Softw 2016;95:51–67. https://doi.org/10.1016/j.advengsoft.2016.01.008.

[26] Kaveh A, Mohammadi S, Hosseini OK, Keyhani A, Kalatjari VR. Optimum parameters of tuned mass dampers for seismic applications using charged system search. Iran J Sci Technol Trans Civ Eng 2015;39:21.

[27] FEMA P 695. Quantification of building seismic performance factors 2009.

[28] Sadek F, Mohraz B, Taylor AW, Chung RM. A method of estimating the parameters of tuned mass dampers for seismic applications. Earthq Eng Struct Dyn 1997;26:617–35.